J. J. Math. and Math. Sci., Vol. **31**, December, 2018, 49-60

SPACE-TIME BASED RLC MODEL FOR GAS FLOW SIMULATION

M. U. AHMMED[1], SHARMIN AKTER[2], SADIYA AKHTER[3] AND KAMRUNNAHAR[4]

[1]*Department of Mathematics, Jahangirnagar University, Dhaka-1342, Bangladesh*

[2]*Department of Mathematics and Natural Sciences, BRAC University, Dhaka, Bangladesh*

[3]*Department of Quantitative Science, International University of Business Agriculture and Technology, Dhaka, Bangladesh*

[4]*Department of Natural Science, BGMEA University of Fashion and Technology, Dhaka, Bangladesh*

Abstract

Flow simulation along human lung of respiratory patient is one of the burning issues in biomechanical engineering field. Fluid flow through 18th generation is our interest of investigation. In this region flow is parabolic and the rate of gas exchange is notable. Lumped parameter model is modified to PDE form to investigate the flow rate $q(x,t)$ instead of $q(t)$. Initially parabolic flow condition is set for numerical simulation. The quasi parabolic flow is examined for a second. However, the flow is found diminished within a few second when preexisting forced is not renewed. This was due to strong resistive force of model channel for dimension $1.2\ \text{mm} \times 4.5\ \text{mm}$.

1. Introduction

The lung is morphologically consisted of a complex network, which is successively bifurcated from trachea to the alveolar zone. Because of its complexities, in-vivo inspection of pulmonary flows is deemed impossible. So, the inspection should be conducted by a suitable modeling, analogical analysis or numerical calculations. Most of the transportation of fluid in physical problem to biological system occur in advection and diffusion process according to the model $q_t + uq_x = Dq_{xx}$, where $q(x,t) =$ flux, D = the rate of diffusion and *u*= the mean flow velocity. Water pollution in oceans, rivers, lakes or ground water and pollution in atmosphere take place continually in surroundings. It is essential to know the contaminant or temperature distribution in the water for safety of the environment [1]. This type of problem describes transport and diffusion process can be modeled using one dimensional advection diffusion equation (ADE). ADE illustrates many quantities such as mass, velocity, heat and energy [2]. Many authors are involved in solving ADE by using finite difference method (FDM).The mathematical model of water pollution is solved using implicit centered difference scheme in space and forward difference method in time by [3]. Aral and Liao [4] solved for two-dimensional transport equation with time dependent dispersion coefficients analytically. Kumar et al. [5]

presented analytical solution of one dimensional ADE with variable coefficients in a finite domain using Laplace transformation. Stability analysis of finite difference scheme for solving ADE is studied by [6-9]. As stated above, most of the works has been done for open channel. But ADE has wide applications in other disciplines too, like biosciences, soil physics, petroleum engineering and chemical engineering. In vivo, fluid (liquid or gas) moves along closed channel and flow might be transported to downstream by advection or spread out by diffusion when unidirectional flow is weaken. For example, a complete cycle of respiration in human lung channel is a consequence of oscillatory flow (advection) and stagnation in transition (diffusion) in nature. Oscillatory flow and mass transport was studied along model channel of human lung by [10, 11]. They simulated governing equations with boundary conditions to show effective diffusion along straight tube. Laminar, turbulent and oscillatory dispersion along a circular channel is calculated by [12]. He established a relation between channel radius and diffusion coefficient. Tanaka et al. [13] examined that a secondary flow during HFOV method ensures effective diffusion in bent and bifurcated tubes than in straight tube. A lamped-parameter model has been developed to study airflow distribution by Elad et al. [14] .The authors also derived the modified time-dependent expressions of resistance and compliance of a single compartment. Numerical analysis of air flow along lung channel with asymmetric compliance was examined experimentally and numerically by Hirahara et al. [15]. We found that the flow for inhomogeneous compliance ratio leads to irreversible flow along lung model. This type of flow effect might be the result of diffusion. Very recently, a numerical study on advection diffusion equation for lung model is published [16]. The effect of inductive time constant is investigated for lung model.

With the above discussions, in this paper, time and space based physical domain is taken in consideration instead of lumped parameter model. Explicit finite difference scheme is employed to solve the computational model. The results for parabolic flow condition is investigated and presented graphically.

2. Anatomy of Human Lung and Parameters

According to the respiratory function and its anatomical configuration, the lung is divided into two regions; air transport and gas diffusion regions. The airways from trachea (G0, G is for generation) to the terminal bronchioles (G16) is bifurcated repeatedly and gas is transported without any gas exchange. Then, the volume is called as the anatomical dead space. Gas diffusion is dominated in the bottom of the lung. The respiratory zone (G17 to G23) having respiratory bronchioles, alveolar ducts and alveolar sacs plays a role of gas exchanger. A numerous networks of tubes from the terminal bronchiole to the most distal alveolus contain about 2.5 to 3 liters of air whereas the standard adult lung contains about 5 liters of air. Active gas mixing and exchange will be expected in the alveolated respiratory region to maintain the effective molecular diffusion.

When we use HFOV for the treatment, an oscillatory flow is induced in the deep region of lung, from G17 to G23. In general, the oscillatory flow is characterized with Stokes layer thickness

$$\delta = \sqrt{\nu / \omega} \tag{1}$$

where ν (= 1.513 $\times 10^{-5}$ m^2/s, 20 degrees in Celsius for air) and ω ($=2\pi f$, f is the frequency) are kinematic viscosity and angular frequency of oscillatory flow, respectively. And also, the flow is represented with two fundamental dimensionless parameters, Reynolds number,

$$Re = UD / \nu \tag{2}$$

and Womersley number

$$\alpha = (D/2)/\delta \tag{3}$$

Re decreases from trachea to bottom, 4000 at the trachea, 30 at terminal bronchus and less than 0.04 in the alveolar region under a normal breathing condition, ω represents the ratio of inertia term to viscous term where the value of ω is important to consider the near wall flow.

3. Quantification of Lung Tree

According to idealization of the human airways, the important non-dimensional parameters for normal breathing condition can be calculated in flow field as depicted in Table 1. The acoustic Reynolds number in this table is a non dimensional quantity based on boundary layer thickness and is defined as

$$\mathrm{Re} = u_{\max} \sqrt{2/\nu\omega}\,.$$

The adult trachea has a mean diameter of 1.8 cm and length of 12 cm. An external pressure of the order of 4 kPa (40 cmH_2O) is sufficient to occlude the trachea. Main, lobar and segmental bronchi are bifurcated from G1 to G4. The trachea bifurcates asymmetrically, with the right bronchus being wider and making a smaller angle with the long axis of the trachea. The small bronchi (G5 to G11) extend through about seven generations with their diameter progressively falling from 3.5 mm to 1 mm. An important change occurs at about the 11th generation where the internal diameter is about 1 mm. The caliber of the airways below the 11th generation is influenced mainly by lung volume. The number of bronchioles from G12 to G14 increases far more rapidly than the calibre diminishes. Therefore, the total cross-sectional area increases until, in the terminal bronchioles (G15),

it is about 100 times the area at the level of the large bronchi. Thus the flow resistance of these smaller air passages (less than 2 mm diameter) is negligible under normal conditions. However, the resistance of the bronchioles can increase to very high values down to the terminal bronchiole. According to the dichotomy model of human lung, the respiratory bronchioles, alveolar ducts and alveolar sacs construct a respiratory zone (G17 to G23) where conduction and diffusion take place in gas transportation. The transition from convection to diffusion occurs at the beginning of respiratory zone. The upper 16 generations make up the conducting zone or dead space. In respiratory zone, there is a gradual increase in number of alveoli so that gas exchange occurs here. The last generation (G23) is filled with alveolar sacs. It is estimated that every alveolar sac is consisted of about 17 alveoli.

As rough approximations it may therefore be assumed that the number of passages in each generation is double that in the previous generation, and the number of air passages in each generation is approximately indicated by 2^n, n be the number of generation. This formula indicates one trachea, two main bronchi, four lobar bronchi, 16 segmental bronchi etc. Pairs of daughter bronchi are often unequal in size and trifurcations may be demonstrated. The adult trachea (G0) and the alveolar sac (G23) have a mean diameter of 1.8cm, 0.04 cm and length of 11cm, 0.05 cm respectively.

For mammals including humans, the respiratory system can be subdivided into an upper respiratory tract and a lower respiratory tract based on anatomical features. The upper respiratory tract includes the nasal passage, pharynx and the larynx, while the lower respiratory tract refers to the portions of the respiratory system from the trachea to the lungs. The respiratory system can also be divided into physiological or functional zones. These include the conducting zone (the region for gas transport from the outside atmosphere to just above the alveoli), the transitional zone and the respiratory zone (the alveolar region where gas exchange occurs). The upper respiratory tract is part of the conducting zone. The upper and lower respiratory tracts make up our whole respiratory system and work in a synchronizing pattern to make it possible to breathe. The lower respiratory tract is a vital system. This tract is responsible for receiving oxygen and distributing it thought-out our whole body through the interface of lung and capillary tube walls. If the lower respiratory tract shuts down, the body can’t receive this vital oxygen and leads to severe brain damage and death.

Table 1: Approximate quantification of the human bronchial system (Weibel's model)

	G	Number	Mean diameter [mm]	Length [mm]	Volume [ml]	Acoustic *R*e	*R*e	*W*o
Trachea	0	1	18.00	120.00	30.54	402.01	1480	2.60
Main Bronchus	1	2	12.20	47.60	11.13	437.55	1092	1.76
Lobar bronchus	2	4	8.30	19.00	4.11	472.68	803	1.20
	3	8	5.60	7.60	1.50	519.17	595	0.81
Segmental bronchus	4	16	4.50	12.70	3.23	402.01	370	0.65
Bronchi w/ cartilage in wall	5	32	3.50	10.70	3.29	332.27	238	0.51
	6	64	2.80	9.00	3.55	259.59	149	0.41
	7	128	2.30	7.60	4.04	192.36	91	0.33
	8	256	1.96	6.40	4.94	132.44	53	0.28
	9	512	1.54	5.40	5.15	107.27	34	0.22
	10	1024	1.30	4.60	6.25	75.26	20	0.19
Terminal bronchus	11	2048	1.09	3.90	7.45	53.53	12	0.16
Bronchiole w/ muscle in wall	12	4096	0.96	3.30	9.78	34.50	6.78	0.14
	13	8192	0.82	2.70	11.68	23.65	3.97	0.12
	14	16384	0.74	2.30	16.21	14.52	2.20	0.11
	15	32768	0.66	2.00	22.42	9.13	1.23	0.10
Terminal bronchiole	16	65536	0.60	1.65	30.57	5.52	0.68	0.09
Respiratory bronchiole	17	131072	0.54	1.41	42.33	3.41	0.38	0.08
	18	262144	0.50	1.17	60.22	1.99	0.20	0.07
	19	524288	0.47	0.99	90.05	1.12	0.11	0.07
Alveolar duct	20	1048576	0.45	0.83	138.42	0.61	0.056	0.07
	21	2097152	0.43	0.70	213.18	0.34	0.030	0.06
	22	4194304	0.41	0.59	326.72	0.18	0.015	0.06
Alveolar sac	23	8388608	0.41	0.50	553.75	0.09	0.008	0.06
Alveoli. 21 per duct		3E+0	0.E+2	0.E+3				

According to the measurement of lung tree and its anatomy the human airways of lung are shown in figure 1. It is drawn by performing calculation of Weibel's real data analysis for adult lung.

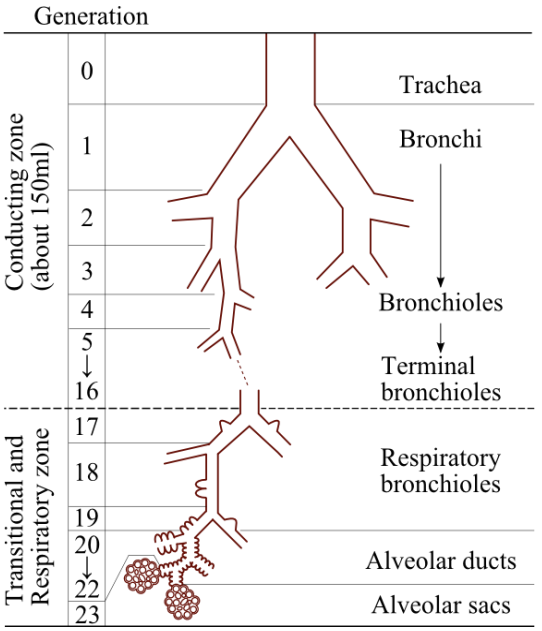

Figure 1: Idealization of the human airways (according to Weibel, 1963)

4. Mathematical Model of the System

4.1: Mathematical Model of Lung Tree

From trachea to alveolar sacs, the lung tree is divided into 23 times and the junction of tree is increased exponentially as in figure 1. The lung tree is formed by bifurcation of each branch and the total number of generation is 23.

The number of branches at n-th generation is

$$N(n) = b^n \tag{4}$$
$$n = \{0, 1, 2, \ldots 23\}$$
$$b = 2(\text{for bifurcation})$$

The gradient of bifurcation at n-th generation is

$$N' = N \ln b \tag{5}$$
$$= rN,\ r = 0.69$$

The average length of each branch is

$$L = \frac{1}{24}\sum_{n=0}^{23} l_n \tag{6}$$

The average diameter of each branch is

$$D = \frac{1}{24}\sum_{n=0}^{23} d_n \tag{7}$$

The average volume of each branch is

$$V = \frac{\pi}{4} L D^2 \tag{8}$$

The total area of entire lung is

$$A = \int_0^n N(n)\, dn + b \tag{9}$$

Where b is the initial area (area of trachea or zero generation).

4.2: Formation of Governing Equation

A model channel of human lung with compliance C (flexibility) and resistance R is taken under consideration. An oscillatory flow with fluid velocity *u* is passing along the model channel and inertial effect L raise. If q(t) is the flow rate and ΔP is the driving force then the lumped parameter model by Elad et al. [14] is

$$L_i \frac{dq_i}{dt} + R_i q_i + \frac{1}{C_i}\int q_i dt = \Delta p \tag{10}$$

Where the flow rate, resistance, inertance and compliance of i-th channel are q_i, R_i, L_i, and C_i respectively, $\Delta P = P_0 \sin(\omega t + \varphi)$ is the driving force for the pressure amplitude, P_0 and $\omega = 2\pi f$ where *f* is the number of oscillation at the inlet of channel.

Differentiating Eqn. (10) and executing some algebra, a second order ODE is obtained which exhibits time varying effect of flow only. It is a crying need to have a flow simulation for spatial and temporal quantities such that $q = q(x,t)$. The following substitutions are integrated for space-time equation of the model.

$$\frac{dq}{dt} = uq_x + q_t$$
$$\frac{d^2q}{dt^2} = u^2 q_{xx} + q_{tt} + 2uq_{tx} \tag{11}$$

In absence of driving force (during transition), Eqn.(2) contributes

$$Lq_{tt} + 2Luq_{tx} + Lu^2 q_{xx} = -q/C - Rq_t - Ruq_x \tag{12}$$

Disregarding the compliance of channel (rigid model), Eqn.(12) becomes

$$aq_{tt} + bq_{tx} + cq_{xx} = dq_t + eq_x \tag{13}$$

Where $a = L, b = 2Lu, c = Lu^2, d = -R$ and $e = -Ru$.

Here $b^2 = 4ac$ confirms that Eqn.(13) is parabolic. Moreover, it befalls parabolic after ignoring mixed term and the rate of flow rate whose effect is unimportant in the system. Since the resistive force is opposite to the main flow, *d* is always positive. According to the above mentioned considerations, the governing equation of the dynamical problem is:

$$q_t + uq_x = Dq_{xx}$$
$$D = Lu^2 / R \tag{14}$$

which is a one dimension advection-diffusion equation with inductive time constant. The first term is local accumulation, the second term is movement by carrying fluid and the last term is movement by random motions in the fluid.

4.3: Computational Model of the System

The unsteady incompressible flow along a rigid channel without driving force and compliance effect is an advection-diffusion Eqn.(14). In physical domain of channel length ($0 \le x \le l$), this one-dimensional transport equation as initial boundary problem can be written as

$$q_t + uq_x = Dq_{xx}$$
$$q(x,0) = q_0(x), \quad 0 \le x \le l \tag{15}$$
$$q(0,t) = g(t), \quad q(l,t) = h(t), \quad 0 < t \le T$$

In order to obtain computational scheme by finite difference method (FDM), we discretize the space-time plane with mesh size $\Delta x \times \Delta t$. Space size and time steps are taken equal individually. The spatial and temporal coordinate at the grid point $q(x_i, t_j)$ is defined as

$$x_i = x_0 + i\Delta x;\ i = 0,1,2,\cdots,m$$
$$t_j = t_0 + j\Delta t;\ j = 0,1,2,\cdots,n$$

The approximate solution at grid points $q(x_i, t_j)$ is $q_{i,j} \in R^n$ so that $q_{i,j} \approx q(x_i, t_j)$.

Employing finite difference scheme with forward time difference, backward space difference and symmetric space difference, the system of equations is

$$\frac{q_{i,j+1} - q_{i,j}}{\Delta t} + \frac{q_{i,j} - q_{i-1,j}}{\Delta x} = \frac{q_{i+1,j} - 2q_{i,j} + q_{i-1,j}}{\Delta x^2}$$

Dropping the truncation error terms and rearranging, we can explicitly solve for time level that implies

$$q_{i,j+1} = sq_{i+1,j} + (1 - r - 2s)q_{i,j} + (r + s)q_{i-1,j}$$
$$\text{for } 1 \le i \le m-1,\ 0 \le j \le n-1 \qquad (16)$$
$$\text{where}, r = u\frac{\Delta t}{\Delta x}, s = \frac{D\Delta t}{\Delta x^2}$$

The von Neumann simultaneous stability condition for the scheme [17] is $r + s \ge 0$ and $1 - r - 2s \ge 0$ which correspond to $0 \le s \le 1/2$ and $-s \le r \le 1 - 2s$. This condition controls the time increment by $\Delta t \le \frac{\Delta x^2}{u\Delta x + 2D}$ where D for rate of mass diffusion and u is the flow speed.

5. Results and Discussions of Parabolic Flow

The numerical experiment is performed for parabolic flow in initial stage along 18th generation of model channel. It is continued for 1 second maintaining parametric conditions of lab experiment. Then the flow conditions are observed in different time fractions for free dynamics, say t = 0, t =1/4, t = 3/8, t=1/2, t=5/8, t = 1 seconds etc. Here T0 is for t = 0, T1 is for t = ¼, T2 is for t = 3/8, T3 is for t = ½, T4 is for t = 5/8, T5 is for t = 1. We observed that the flow rate is first increased and then decreased to zero for the change of time within one second due to the effect of high resistance of the narrow and compliant channel as shown in figure.2.

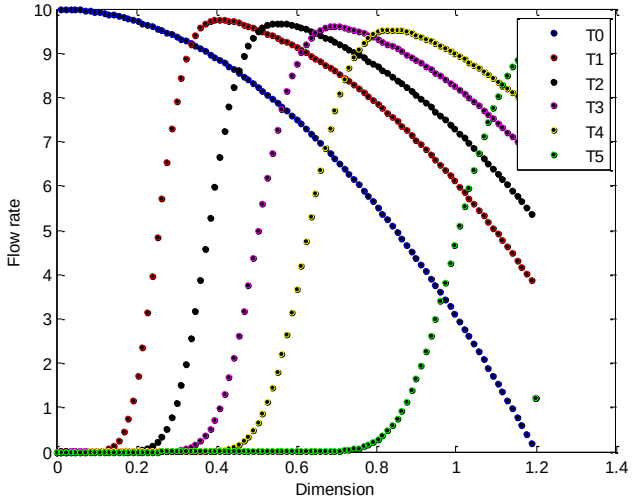

Figure 2: Flow behavior in 18th generation of model in 1second

If the experiment is continued for 6s, the flow rate seems to be constant as depicted in figure 3. . Because, the momentum is finite and is not being renewed by any external force and the flow will be opposed by resistance and recoil force (compliance) of alveoli. It is also found that the flow rate tends to zero. The numerical experiment shows that the only driving force which keeps some flow at this phase is internal force due to the inertial effect. This momentum of flow arose by virtue of the pre-existing velocity with which the experiment was started. Since this momentum is finite and is not being renewed by any external force, it is ultimately exhausted and the fluid comes to rest and the flow rate becomes zero.

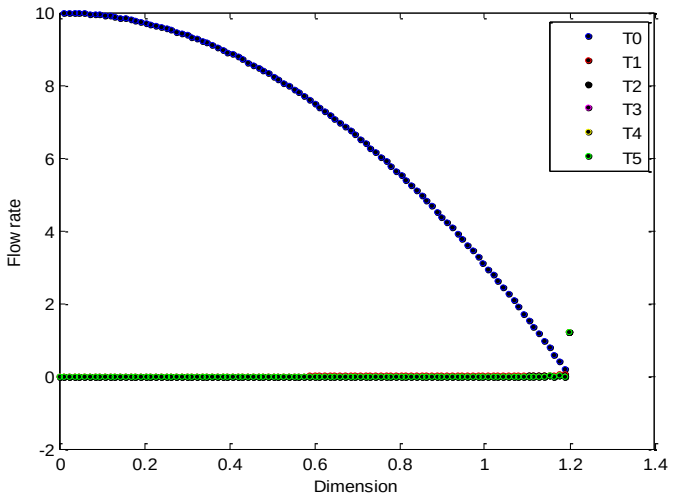

Figure 3: Flow behavior in 18th generation of model in 6 seconds.

6. Conclusion

We conduct the numerical experiment for air flow simulation along human lung of 18^{th} generation. For this, the initial flow condition is taken parabolic. Before numerical simulation, the governing equation of lumped model is introduced in PDE governing form. Explicit finite difference scheme is incorporated to compute the mathematical model. Three flow phenomena are tasted entire the experiment such as parabolic flow (initially), quasi parabolic flow (within a second) and constant flow (within a few second). Also, the zero flow is evident for time being due to free dynamics.

References

1. .G. Koutitas, 'Elements of computational hydraulics', Pentech Press, London, UK, 1983.

2. B.J. Noye, 'Numerical solution of partial differential equations' Lecture notes, 1990.

3. F.B. Agusto, O.M. Bamigbola, 'Numerical treatment of the mathematical models for water pollution', Research J. Appl. Sci. 2(5), 548-556, 2007.

4. M.M. Aral and B. Liao, 'Analytic solutions for two-dimensional transport equation with time dependent dispersion coefficients', J. Hydrol. Eng., 1(1), 20-32, 1996.

5. A. Kumar, D. Kumar and N. Kumar, 'Analytical solution of one dimensional advection diffusion equation with variable coefficients in a finite domain', J. Earth. Syst. Sci. 118(5), 539-549, 2009.

6. K.W. Morton, 'Stability of finite difference approximations to a diffusion-convection equation', Int. J. Numerical Methods in Eng., 15(5), 677-683, 1980.

7. L.F. Leon, P.M., Austria, 'Stability criterion for explicit scheme on the solution of advection-diffusion equation', Maxican Institute of Water Technology.

8. T.M.A.K. Azad and L.S. Andallah, 'Stability analysis of finite difference schemes for an advection diffusion equation', Bangladesh J. Sci. Res. 29(2), 143-151, 2016.

9. H. Karahan, 'Unconditional stable explicit finite difference technique for the advection-diffusion equation using spread sheets', Advances in Eng. Software, 38(2), 80-86, 2007.

10. D.M. Eckmann, J.B. Grotberg, 'Oscillatory flow and mass transport in a curved tube', *J. Fluid Mech.,* 188, 509– 527, 1988.

11. H. Fujioka, K. Oka, and K. Tanishita, 'Oscillatory flow and gas transport through a symmetrical bifurcation', J. Biomechanical. Eng., 123, 145–153, 2001.

12. H.K. Chang, 'Mechanisms of gas transport during ventilation by high-frequency oscillation', J. Appl. Physiology 56(3): 553-563.

13. G. Tanaka, T. Ogata, K. Oka, and K. Tanishita, 'Spatial and temporal variation of secondary flow during oscillatory flow in model human central airways'J. Biomechanical. Eng., 121, 565–573, 1999.

14. D. Elad, A. Shochat and R.J. Shiner, 'Computational model of oscillatory airflow in a bronchial bifurcation' Respiration Physiology, 112, 95-111, 1998.

15. H. Hirahara, K. Iwazaki, M.U. Ahmmed, M. Nakamura, 'Numerical analysis of air flow in dichotomous respiratory channel with asymmetric compliance under HFOV condition' Journal of Fluid Science and Technology, 6(6), 932-948, 2011.

16. M. U. Ahmmed and M. Khatun, ' Numerical study on advection diffusion equation for human lung model channel, U. J. Sci. Engg., 8(1), 29-36 , 2017.

17. D.M. Causon and C.G. Mingham, Intoductory Finite Difference Method for PDE.